

Effect of friction on energy release rate for interfacial cracks in gravity dams

J.M.Chandra Kishen & V.Sujatha

Dept. of Civil Engineering, Indian Institute of Science, Bangalore, 560 012, India

ABSTRACT: The combined compression and shear loading in dams causes the crucial rock concrete interfacial crack faces to come in contact. Hence sizeable contact zone emerge near the crack tip. Frictional contact of the crack surfaces cannot be neglected if the contact zones are finite. The frictional contact alters the stress singularity to become either weak or strong than the inverse square root singularity as observed in homogeneous crack problems. Consequently, the strain energy release rate as conventionally defined, either vanishes or becomes unbounded and thus cannot be used as a fracture parameter. A computational scheme has been suggested and implemented to include the effect of friction associated with the sliding of crack surfaces and compute the energy dissipated during crack propagation

1 INTRODUCTION

The interface between two dissimilar materials is one of the potential sites of crack occurrence and propagation in many structures. In concrete gravity dams, an interface is formed between the concrete superstructure and rock foundation. The tools of fracture mechanics have been applied to study this rock-concrete interface assuming stress free crack surfaces (Chandra 1996 & Chandra et al. 2001). In real life situation, because of combined compression and shear loading, the crack faces come in contact so that sizeable contact zone emerge near the crack tip. Frictional contact of the crack surfaces cannot be neglected if the contact zones are finite. The frictional contact alters the stress singularity to become either weak or strong (Sun & Qian 1998) than the inverse square root singularity as observed in homogeneous crack problems. Consequently, the strain energy release rate as conventionally defined, either vanishes or becomes unbounded and thus cannot be used as a fracture parameter.

In this work, an attempt is made to include the effect of friction associated with the sliding of crack surfaces and compute the energy dissipated during crack propagation. Finite element analysis is performed on an existing dam to highlight the effect of friction on the energy release rate along the rock-concrete interface.

2 STRAIN ENERGY RELEASE RATE

2.1 Formulation

Cracks in homogeneous media invariably show square root singularity irrespective of the presence or absence of friction. But for bi-material case the singularity index λ is related to the coefficient of friction μ as (Comninou 1997b; Sun & Qian 1998)

$$\cot \lambda \pi = \mu \beta \quad (1)$$

where β is one of the Dunders' elastic parameters (Dunders 1969). A crack tip is said to have a weak singularity if λ is less than 0.5 and strong singularity when λ is greater than 0.5. When λ is equal to 0.5, the singularity is termed as square root singularity as existing in homogeneous material. It can be seen from Equation 1, that the value of λ depends on values of β and μ . It is obvious that λ is 0.5 if β or μ is zero, which corresponds to a homogeneous media or a frictionless condition, respectively. A weak singularity ($\lambda < 0.5$) at the crack tip is predicted by Equation 1, when β is greater than zero whereas when β is less than zero a strong singularity ($\lambda > 0.5$) exists at the crack tip.

The general form of the near tip stress field of both strong and weak singularities for a bi-material

interface crack are given by Sun & Qian (1998,1998) as,

$$\sigma_{xy}(r,0) = K_{II} (2\pi r)^{-\lambda} \quad (2)$$

$$\sigma_{xy}(r,\pm\pi) = K_{II} \cos \lambda\pi (2\pi r)^{-\lambda} \quad (3)$$

$$\sigma_{xy}(r,\pm\pi) = -K_{II} \beta \sin \lambda\pi (2\pi r)^{-\lambda} \quad (4)$$

and the relative crack surface sliding displacement as,

$$\Delta u_x(r) = u_x(r,\pi) - u_x(r,-\pi) \quad (5)$$

$$= [K_{II} \gamma \sin \lambda\pi / 2(1-\lambda)(2\pi r)^\lambda] r^{1-\lambda} \quad (6)$$

where the generalised stress intensity factor K_{II} is defined as

$$K_{II} = \lim_{r \rightarrow 0} (2\pi r)^\lambda \sigma_{xy}(r,0) \quad (7)$$

and

$$\gamma = \left[\frac{(3-4\nu_1)(1-\beta) + (1+\beta)}{2\mu_1} \right] + \left[\frac{(3-4\nu_2)(1+\beta) + (1-\beta)}{2\mu_2} \right] \quad (8)$$

The above solutions are based on the assumption that the crack surfaces slide and the normal and shear stress behind the crack tip follow the Coulomb frictional law, i.e.,

$$\sigma_{xy}(r,\pm\pi) < 0 \quad (9)$$

$$\sigma_{xy}(r,\pm\pi) = -\mu \sigma_{yy}(r,\pm\pi) \quad (10)$$

$$\text{sgn}(\mu) = \text{sgn}(\Delta u_x) \quad (11)$$

The strain energy released for a crack extension Δa can be obtained using Irwin's crack closure integral (Irwin 1957). The energy released during the extension of a crack by an infinitesimally small value of Δa is the same as that required to close the crack back to its original length. Strictly, the work done to close the crack back to its original length should be the product of stress distribution over the crack extension length Δa ahead of the tips of the original crack before crack extension and the crack face displacements over the length behind the tips of the extended crack after crack extension. This would call for two analyses, one with a crack length of a

and the other with a crack length of $a+\Delta a$. When the crack surfaces are not in contact (Irwin 1957),

$$G_I = \lim_{\Delta a \rightarrow 0} \frac{1}{2\Delta a} \int_0^{\Delta a} \tau_{xy}(\Delta a - r) \bar{v}(r) dr \quad (12)$$

$$G_{II} = \lim_{\Delta a \rightarrow 0} \frac{1}{2\Delta a} \int_0^{\Delta a} \tau_{xy}(\Delta a - r) \bar{u}(r) dr \quad (13)$$

When the crack surfaces are in contact behind the crack tip, only mode II is present, and the total strain energy release rate associated with Δa is (Sun & Qian 1998,1998)

$$\hat{G}_{II}(\Delta a) = \frac{1}{2\Delta a} \int_0^{\Delta a} [\sigma_{xy}(r,0) - \sigma_{xy}(\Delta a - r,\pi)] \Delta u_x(\Delta a - r) dr \quad (14)$$

$$= \frac{K_{II}^2 \sin \lambda\pi}{4(1-\lambda)(2\pi)^{2\lambda}} \Delta a^{1-2\lambda} \left[\frac{\Gamma(2-\lambda)\Gamma(1-\lambda)}{\Gamma(3-2\lambda)} - \frac{\cos \lambda\pi}{2(1-\lambda)} \right] \quad (15)$$

where Γ is a gamma function.

The conventional strain energy rate is defined as,

$$G = \lim_{\Delta a \rightarrow 0} \hat{G}_{II}(\Delta a) \quad (16)$$

In the crack closure integral of Equation 14, the term $\sigma_{xy}(r,0)$ is the interfacial shear stress ahead of the crack tip, and $\sigma_{xy}(\Delta a-r,\pi)$ is the frictional shear stress behind the crack tip. During the crack extension of Δa , the shear stress initially ahead of the crack tip reduces to that of the frictional shear stress behind the crack tip after the assumed crack extension. Thus, the strain energy release rate of Equation 14 can be interpreted as the total energy release rate less the frictional energy dissipation rate. $\hat{G}_{II}(\Delta a)$ can be regarded as the elastic energy that is expended in propagating the crack by Δa . For a frictionless interfacial crack ($\mu=0$), $\lambda=0.5$, we obtain from Equation 15,

$$\hat{G}_{II}(\Delta a) = \frac{K_{II}^2}{4\gamma} \quad (17)$$

which is independent of Δa . The conventional definition of strain-energy release rate thus exists. However, it can be seen from Equation 14 that for a frictional interfacial crack, the strain energy release rate $\hat{G}_{II}(\Delta a)$ vanishes as $\Delta a \rightarrow 0$ due to the weak singularity ($\lambda < 0.5$). On the other hand, a strong singularity ($\lambda > 0.5$) causes $\hat{G}_{II}(\Delta a)$ to become unbounded as $\Delta a \rightarrow 0$. The decreasing behaviour of the strain energy release rate was also noticed by Stringfellow & Freund (1993) who computed the J-integral for the frictional sliding fracture in a thin film on a sub-

strate. Deng (1994) later showed that the path independence of the J-integral no longer exists due to the crack surface traction resulting from friction, and the J-integral for a vanishingly small contour becomes zero indicating that the strain energy release rate vanishes. Consequently, the conventionally defined strain energy release rate (which requires $\Delta a \rightarrow 0$) does not exist if $\lambda \neq 0.5$ and hence cannot be used as a parameter in the fracture criterion. On the other hand, for $\Delta a = \Delta a_0 \neq 0$, $\hat{G}_{II}(\Delta a_0)$ is uniquely related to the stress intensity factor K_{II} and, thus, to the near tip stress field. It is assumed that Δa used for calculating strain energy release rates satisfy $\Delta a > r_c$, where r_c is the oscillation zone (Rice 1988). Thus, by selecting a proper characteristic crack closure distance Δa_0 , it seems possible to use $\hat{G}_{II}(\Delta a_0)$ as a fracture parameter when friction is present. It should be noted that the simple relation between strain energy release rate, strain energy and work done in linear elastic fracture mechanics are no longer valid in the presence of friction (Sun & Qian 1998).

2.2 Computation

As the crack propagates by an amount Δa , it may open completely, close completely or partially close. When the crack opens completely (no contact), the strain energy released are the conventional mode I G_I and mode II G_{II} . No energy is dissipated due to friction. It is well known that the total energy release rate is

$$G_T = G_I(\Delta a) + G_{II}(\Delta a) \quad (18)$$

As discussed in the previous sections, when the crack is in closed mode, the strain energy released is defined as \hat{G}_{II} . The total energy release rate is given as (Sun & Qian 1998),

$$G_T = \hat{G}_{II}(\Delta a) + G_d(\Delta a) \quad (19)$$

where $G_d(\Delta a)$ is the frictional dissipation energy. When the crack is partially closed all the components may be present. In the open zone, the conventional G_I and G_{II} and in the closed zone, \hat{G}_{II} and G_d exists. For clarity the G_{II} in open zone has been denoted as \bar{G}_{II} even though they are one and the same (conventional mode II strain energy release rate). Thus, the total mode II strain energy release rate, $G_{II} = \bar{G}_{II} + \hat{G}_{II}$. The total energy release rate in this case is given as

$$G_T = G_I(\Delta a) + \bar{G}_{II}(\Delta a) + G_d(\Delta a) \quad (20)$$

2.2.1 Strain energy release rate (SERR)

The stress and displacement distribution in the elements ahead and behind the crack tip respectively can be assumed in simple polynomial forms. The stress in Equations (12, 13 & 14) can be expressed in terms of the nodal forces ahead of the crack tip and the displacement distribution in terms of the nodal

displacements behind the crack tip to evaluate the SERR components from the finite element analysis. Analytical solutions for the interfacial cracks with frictional sliding are extremely difficult to obtain. A finite element procedure is developed to calculate the strain energy release rates and the energy dissipation due to friction $G_d(\Delta a)$ during crack extension. Using Irwin's crack closure concept, the expressions for G_I , G_{II} and \hat{G}_{II} for eight noded quadrilateral element are

$$G_I(\Delta a) = \frac{1}{2\Delta a} [F_{ym}^1(\Delta u_{ym}) + F_{yn}^1(\Delta u_{yn})] \quad (21)$$

$$G_{II}(\Delta a) = \frac{1}{2\Delta a} [F_{xm}^1(\Delta u_{xm}) + F_{xn}^1(\Delta u_{xn})] \quad (22)$$

$$\hat{G}_{II}(\Delta a) = \frac{1}{2\Delta a} \left[(F_{xm}^1 - \mu F_{ym}^1)(\Delta u_{xm}) + (F_{xn}^1 - \mu F_{yn}^1)(\Delta u_{xn}) \right] \quad (23)$$

where F_{xm}^1 , F_{xn}^1 and F_{ym}^1 , F_{yn}^1 are the respective nodal horizontal and vertical forces ahead of the crack tip in the loaded medium. The superscript 1 refer to the state before crack extension. Δu_{xm} , Δu_{xn} and Δu_{ym} , Δu_{yn} are the relative sliding and opening of the nodes and μ is the coefficient of friction. The elastic restoring force at node m is $(F_{xm}^1 - \mu F_{ym}^1)$. m refers to the edge node and n refers to the intermediate node.

2.2.2 Dissipation Energy

To facilitate friction, interface element 2-D GAP/FRICTION elements are used. During the assumed crack extension, the total dissipation energy associated with the crack surface friction is given by

$$G_d(\Delta a) = G_d^N(\Delta a) + G_d^e(\Delta a) \quad (24)$$

where $G_d^N(\Delta a)$ is the portion of the dissipation energy rate produced by the newly formed crack surface, and $G_d^e(\Delta a)$ is the portion produced by the existing crack surfaces that are in contact. We have

$$G_d^N(\Delta a) = \frac{1}{2\Delta a} \left[(\mu F_{ym}^1 + \mu F_{ym}^2)(\Delta u_{xm}) + (\mu F_{yn}^1 + \mu F_{yn}^2)(\Delta u_{xn}) \right] \quad (25)$$

where F_{ym}^1 and F_{yn}^1 are the vertical crack tip nodal forces. The superscript 1 and 2 refer to the state before and after crack extension respectively. The calculation of $G_d^e(\Delta a)$ is similar to that of $G_d^N(\Delta a)$ and should include all the nodes in the contact region before crack extension.

3 APPLICATION TO CONCRETE GRAVITY DAM

The method formulated in above section is used to separate the energy dissipation due to friction from

the total energy release rate as the crack propagates, under the LEFM (linear elastic fracture mechanics) regime, to give an account of the the effect of friction on the reduction of the strain energy release rate at the rock concrete interfacial crack.

3.1 Description of the Dam

The dam used for the analyses is a gravity dam constructed during the thirties (Chandra 1996). It is 176 feet high and has 53 monoliths, with a crest elevation of 1535 feet. The probable maximum flood (PMF) elevation is at 1555.8 feet. The cross section of the dam is shown in Figure 1. The material properties of rock and concrete are given in Table 1.

Table 1. Material properties of rock and concrete

Material	Weight density	Elastic modulus	Poissons ratio
	lbs/ft ³	psi	
Concrete	150	4.867e+6	0.255
Rock	0	3.952e+6	0.165

The following loads are used in the analysis:

- Hydrostatic load.
- Body forces due to the self weight of the dam.

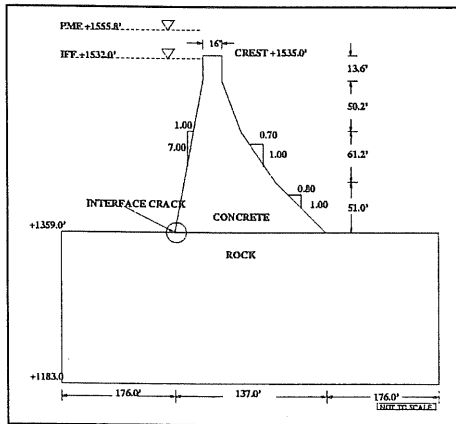


Figure 1. Simplified geometry of the Dam

3.2 Finite Element Model

The rock foundation is modeled as a rectangular block 489 feet wide and 176 feet high. The dam is tances from the upstream edge of the rectangle to the heel of the dam and from the toe of the dam to the downstream edge of the rectangle are both 176 feet. The unit weight of the rock foundation is neglected so that the stresses computed in the foundation are those caused by the dam and the reservoir (i.e. insitu stresses are neglected). An initial notch length of 10

feet is considered and the number of gap elements used over this length is 20. To accommodate crack propagation along the base of dam, the portion of the mesh for the dam and foundation adjacent to the base is refined with coarser mesh elsewhere. The crack is simulated by providing duplicate nodes on either side of the interface. The nodes on the vertical surfaces of the foundation, on both the upstream and downstream ends, are constrained against displacement in the horizontal direction. The nodes on the bottom horizontal direction surface of the foundation are constrained against displacement in the vertical direction. Analysis is carried over for three different values of friction namely, 0°, 52° and 63° to study the effect of friction on the interface crack propagation behaviour.

4 RESULTS AND DISCUSSIONS

Figure 2, shows the variation of the relative normal crack face displacement with crack length for the upstream elevation of 184 feet. When the friction is zero, it is seen that the crack closes right from the heel of the dam for a crack length of 15 feet (since Δu_y is zero). But for smaller crack length ($a < 15$ feet), there is a small crack open zone. Analysis was done for crack lengths greater than 15 feet and the same was observed. But in the case where friction is introduced the crack never closes upto a certain length from the heel for any crack length. As seen in the figure, for $\phi = 52^\circ$ and 63° this length is constant, indicating that the open zone size remains the same for any value of friction. This observation was also made by Sun & Qian (1998).

Figure 3, shows the variation of G_I , G_{II} , G_d and G_T as a function of crack length and friction at an upstream height of 184 feet. It may be mentioned here that for the frictionless case G_T is the sum of G_I and G_{II} whereas in the case with friction, G_T is the sum of G_I , G_{II} and G_d , where G_d is the energy dissipated due to friction. It is seen that the total energy release rate G_T increases with the crack length when the angle of internal friction is zero and decreases for non zero values of friction. Further, as the value of friction increases the total energy release rate decreases considerably. Thus, friction reduces the energy release rate for increasing crack length. From the results of the status of gap elements used to model the crack, the zones of sliding and sticking are indicated in Figure 3. It is seen that the total energy release rate drops down drastically in the large sliding zone. In the zone of large sticking the drop in the total energy release rate is less. Hence, in the presence of friction both G_{II} and G_d contribute in reducing the G_T .

Figure 4, shows the variation of the relative normal crack face displacement with crack length for the water elevation of 209 feet. It can be seen for the

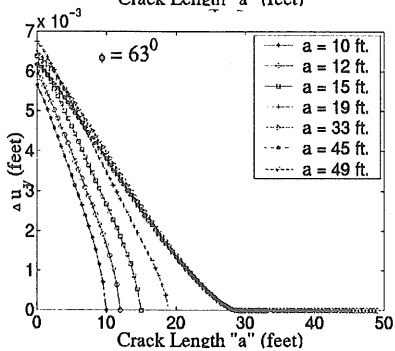
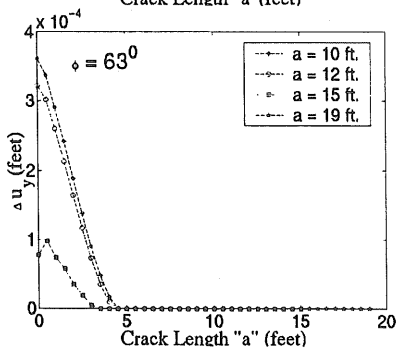
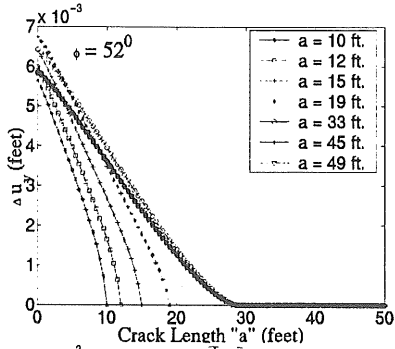
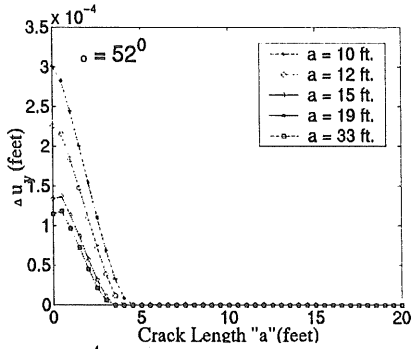
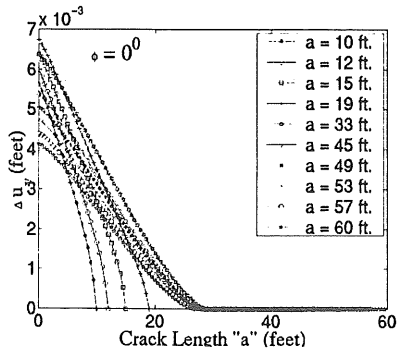
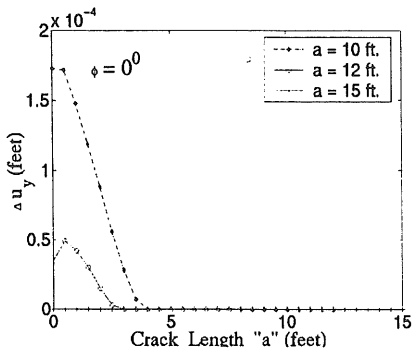


Figure 2. Relative normal crack displacements at the water elevation of 184 feet for different ϕ values

Figure 4. Relative normal crack displacements at the water elevation of 209 feet for different ϕ values

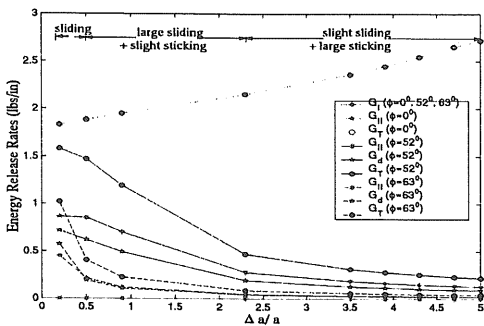


Figure 3. Variation of G_I , G_{II} , G_III and G_{IV} with crack length for water elevation of 184 feet

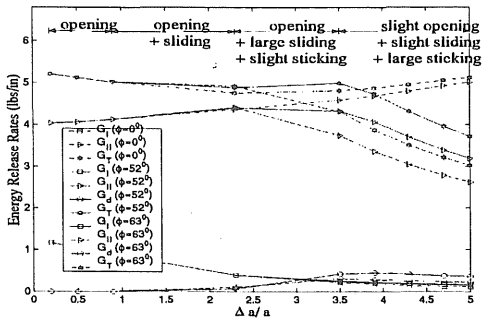


Figure 5. Variation of G_I , G_{II} , G_d and G_T with crack length for water elevation of 209 feet

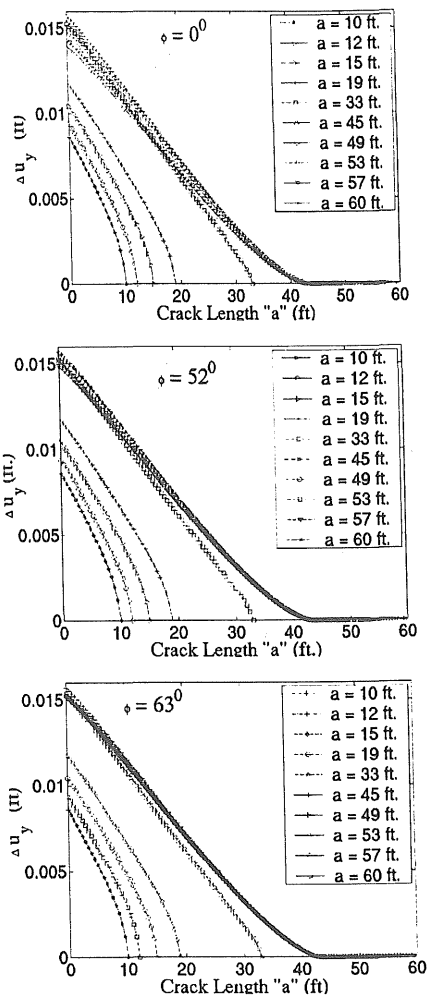


Figure 6. Relative normal crack displacements at the water elevation of 221 feet for different ϕ values

frictionless case that crack faces are open to a certain distance from the heel of the dam. The crack faces starts closing at the crack length of 33 feet. This indicates that the hydrostatic loading tries to open up the crack. As the crack length increases the crack tries to close due to gravity load of dam. It is also observed that the open crack zone at a particular crack length is constant independent of the frictional level.

Figure 5, shows the variation of G_I , G_{II} , G_d and G_T with crack length and friction at the upstream height of 209 feet. The opening, sliding and sticking mode have been shown from the results of gap element used to model the crack. It is seen that initially the crack is in opening mode till $\Delta a/a = 1$. So, the energy values are coincident for all values of ϕ . G_I values are much less than G_{II} values, indicating the predominance of shear. G_I is seen to decrease as the crack length increases. The decrease is more in the zone of sliding. The value of G_T and G_{II} increases with the crack length for the frictionless case. But for the frictional case, both G_T and G_{II} values drop considerably in the sliding zone. G_d is seen to increase in the sliding zone. It becomes more or less constant in the large sticking zone for both the values of ϕ . Thus, G_d and G_{II} both contribute to the decrease in the total energy in the presence of friction.

Figure 6, shows the variation of the relative normal crack face displacement with crack length for the water elevation of 221 feet. It is observed that the crack never closes completely for frictionless and frictional case. This is because the hydrostatic load tries to open up the crack. The crack starts closing at the crack length of 45 feet. It is also observed that the open crack zone constant irrespective of the value of friction.

Figure 7, shows the variation of G_I , G_{II} , G_d and G_T with crack length and friction at the upstream height of 221 feet. It is obvious from the plot that the crack starts sliding at $\Delta a/a = 3.5$. G_d is zero till this point since the crack is in an open state. In this re-

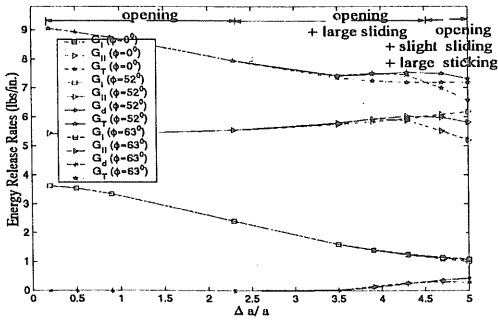


Figure 7. Variation of G_I , G_{II} , G_d and G_T with crack length for water elevation of 221 feet

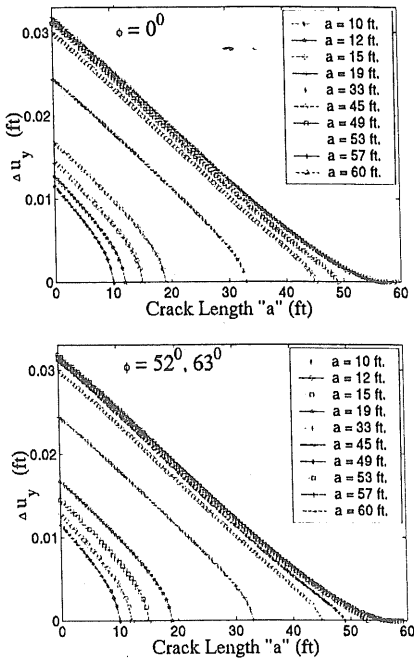


Figure 8. Relative normal crack displacements at the water elevation of 234 feet for different ϕ values

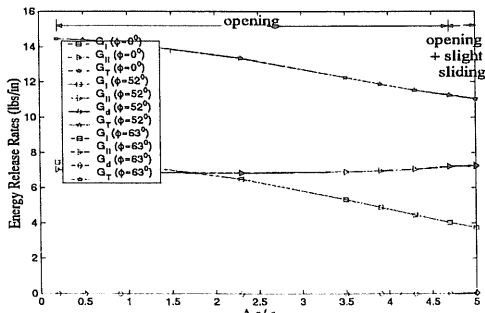


Figure 9. Variation of G_I , G_{II} , G_d and G_T with crack length for water elevation of 234 feet

gion G_I , G_{II} and G_T values are coincident for the different values of friction. Thus friction has no role in an open crack. As the crack starts sliding G_d increases. In the large sliding zone, G_d of $\phi = 63^\circ$ is greater than that of 52° . But in the large sticking zone the nature is reversed and G_d is nearly constant. It can be seen that G_T decreases till $\Delta u/a$ is 3.5 and then it is nearly constant for the frictionless case. In the sliding zone, G_T for $\phi = 52^\circ$ increases slightly and then decreases. The drop in G_T is pronounced in this zone for $\phi = 63^\circ$. Similar behaviour is observed for G_{II} in the sliding zone. Thus larger the frictional value more is the drop in energies. G_I is nearly having the same values for different ϕ . The zones of opening, sliding and sticking have been indicated in the Figure 7, from the results of the status of gap element

Figure 8, shows the variation of the relative normal crack face displacement with crack length for the water elevation of 234 feet. Analysis was done for $\phi = 0^\circ, 52^\circ$ and 63° . It was observed that the crack is in open state throughout except at a distance of $\Delta u/a$, 4.7 to 5. As the crack is in open state, all the three cases showed same nature of relative normal displacement curve.

Figure 9, shows the variation of G_I , G_{II} , G_d and G_T with crack length and friction for water elevation of 234 feet. It can be clearly observed that the G_I , G_{II}

and G_T are coincident for different values of ϕ . There is a small values of between $G_d \Delta a/a$, 4.7 to 5. As the crack length increases G_T decreases. It is also observed that G_I decreases and G_{II} increases as the crack length increases. Thus tension is seen to dominate initially. But as the crack length increases shear mode dominates. This is due to the tendency of the crack to close due to gravity load of dam as the crack length increases.

5 CONCLUSIONS

The main conclusions from this study are:

- In the absence of friction, the total energy release rate remains constant as long as the crack lies within the interface. For low water elevations, irrespective of the value of friction, there is always an open crack zone upto a certain constant length from the heel of the dam. In the absence of friction, this zone exists only for small crack length and is absent for longer crack lengths.
- The total energy release rate increases with the crack length for a frictionless case and decreases with the crack length for frictional case. The frictional energy dissipation contributes to the decrease in the total energy. As the value of friction increases, the total energy release rate decreases considerably. Thus, friction reduces the energy release rate for increasing crack length. This is not applicable for large water elevations since the crack has a tendency to open and the friction plays no role for an open crack.

REFERENCES

- Ayari, M.L. & Saouma, V.E. 1990. A fracture mechanics based seismic analysis of concrete gravity dams using discrete cracks, *Engg. Frac. Mech.* 35 (1-3): 587-598
- Cervera, M., Oliver J., Herrero, E. & Onate, E. 1990. A computational model for progressive cracking in large dam due to swelling of concrete, *Engg. Frac. Mech.* 35(1-3): 573-585
- Chandra, Kishen J.M. 1996: Interface cracks: Fracture mechanics studies leading towards safety assessment of dams, *PhD thesis, Dept. of Civil, Environmental & Architectural Engg., University of Colorado, Boulder*
- Chandra, Kishen J.M. & Singh, K.D 2001: Stress intensity factors based fracture criterion for kinking and branching of interface crack: application to dams, *Engg. Frac. Mech.* 68(2): 201-219
- Comninou, M. 1977b. Interface crack with friction in the contact zone, *Jl. App. Mech.* December: 780-781
- Deng 1994. An asymptotic analysis of stationary & moving cracks with frictional contact along bi-material interfaces and in homogeneous solids, *Int. Jl. of Solids and Structures* 31(17): 2407-2429
- Dunders, J. 1969. Edge bonded dissimilar orthogonally elastic wedges under normal and shear loading, *Jl. of App. Mech.* 36(1): 650-652
- Ingraffea, A.R. et al. (ed.: Shah-S.P. & Swartz S.E.) 1987. Computer simulation of cracking in a large arch dam downstream side cracking, *SEM/RILEM In. Conf. on Frac. of Concrete and Rock*, Houston, Texas, June: 334-342
- Ingraffea, A.R. 1990. Case studies of simulation of fracture in concrete dams, *Engg. Frac. Mech.* 35(1-3): 553-564
- Irwin, G.R. 1957. Analysis of stresses and strains near the end of a crack traversing a plate, *Jl. of App. Mech.* 24(3): 361-364
- Plizzari, G.A. 1997. LFM applications to concrete gravity dams, *Jl. of Engg. Mech.* August: 808-815
- Rice, J.R. 1988. Elastic fracture mechanics concepts for interfacial cracks, *Jl. App. Mech.* March: 98-103
- Saouma, V.E. et al. (ed.: Shah S.P. & Swartz S.E.) 1987. Fracture mechanics of concrete gravity dams, *SEM/RILEM In. Conf. on Frac. of Concrete and Rock*, Houston, Texas June: 311-333
- Stringfellow, R.G. & Freund, L.B. 1993. The effect of interfacial friction on the buckle-driven spontaneous delamination of a compressed thin film, *Int. Jl. of Solids and Structures* 30(10): 1379-1395
- Sun, C.T. & Qian, W. 1998. A treatment of interfacial cracks in the presence of friction, *Int. Jl. of Fracture* 94: 371-382
- Sun, C.T. & Qian, W. 1998. Frictional interfacial crack under combined shear and compressive loading, *Composites Science and Technology* 58: 1753-1761